

TOWARDS A EUROPEAN COMPREHENSIVE SEISMIC MODEL (ECOS)

Andreas Fichtner¹ & Jeannot Trampert¹ in collaboration with

Antonio Villaseñor², Erdinc Saygin³ & Tuncay Taymaz⁴

1: Department of Earth Sciences, Utrecht University, Utrecht, The Netherlands
 2: Department of Geophysics and Tectonics, Institute of Earth Sciences „Jaume Almera“, CSIC, Barcelona, Spain
 3: Research School of Earth Sciences, The Australian National University, Canberra, Australia
 4: Department of Geophysical Engineering, Istanbul Technical University, Istanbul, Turkey

Abstract

We report on the progress of a long-term project that aims at the construction of a comprehensive seismic model of the European crust and upper mantle with a maximum resolution on the order of 10 km in areas where dense regional data sets are available. The present early-stage model is based on full seismic waveforms in the period range from 50 - 300 s, and it reveals the anatomy of intermediate-scale features such as the Pannonian Basin, the Hellenic subduction zone and the Iceland plume. A conservative and preliminary resolution analysis indicates that the resolution length throughout most of central Europe is around 400 km. Furthermore, the model explains waveforms that were not included in the inversion within the expected errors. The next steps consist in the incorporation of regional data, starting with the dense networks in Spain and Turkey.

1. Introduction

The main objective of the ECOS project is to use **full waveform tomography** to compute a **multi-scale model** of the European upper mantle, with a **lateral resolution** ranging between ≈ 1000 km in poorly covered regions to ≈ 10 km in areas where **dense regional data sets** are available.

This is intended

- (1) to provide insight into the complex tectonic structure and evolution of Europe (see figure 1 for an overview of surface tectonic features),
- (2) to establish links between seismic heterogeneities and surface geochemical signatures, and
- (3) to allow for (finite) seismic source inversions that account for 3D heterogeneous Earth structure.

The project is in a comparatively early stage where a long-period model is available, and where regional data sets are about to be incorporated.

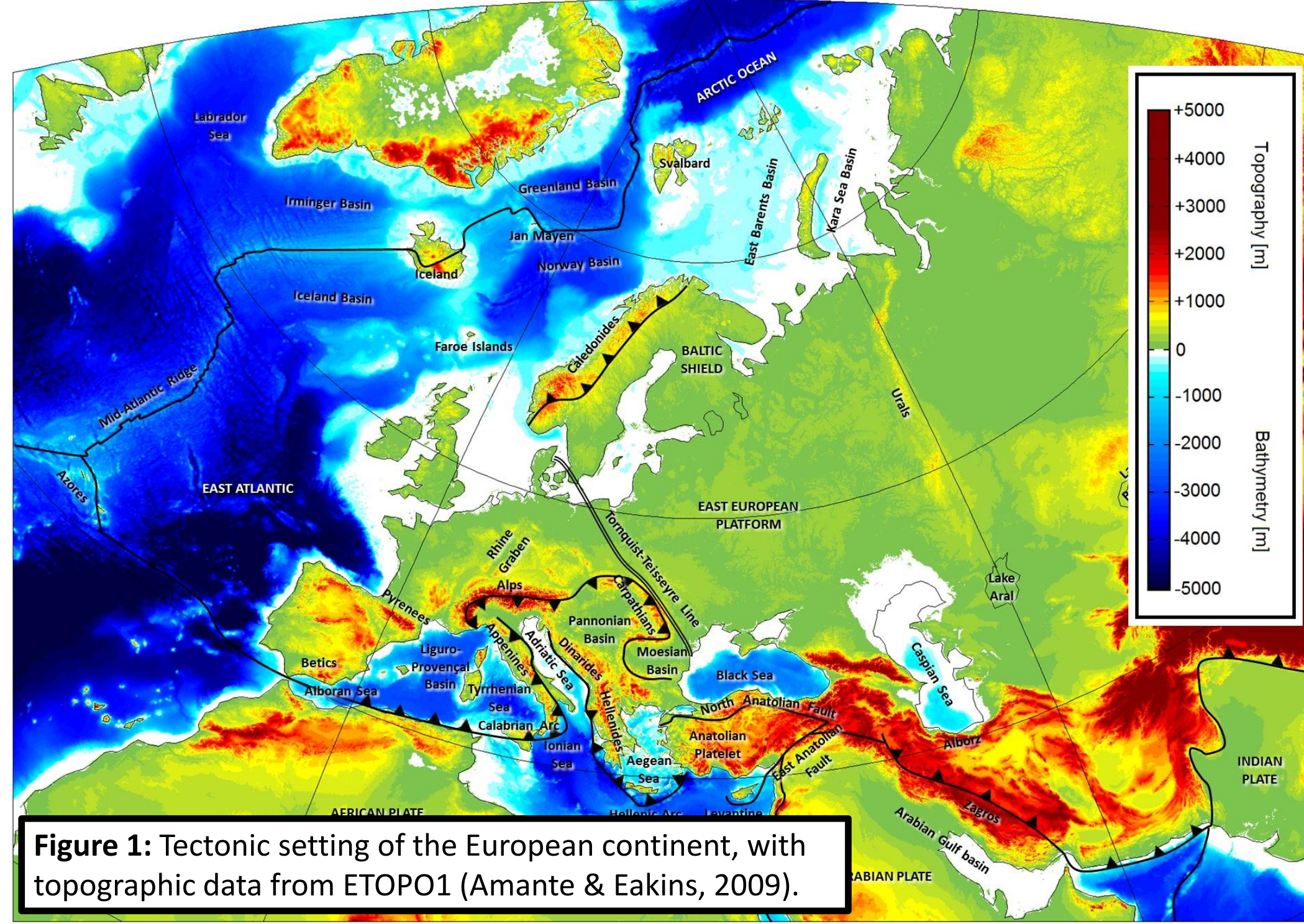


Figure 1: Tectonic setting of the European continent, with topographic data from ETOPO1 (Amante & Eakins, 2009).

2. Data and Method

Data: ≈ 7000 three-component seismograms from 52 events, period range: 50-300 s

Forward problem: Spectral-elements in a spherical section (Fichtner & Igel, 2008)

Misfits measure: Time-frequency phase misfits (Fichtner et al., 2009)

Optimisation: Adjoint-based conjugate gradients

Initial model:

- elastic: v_s : S20RTS (Ritsema et al., 1999), v_p scaled (Ritsema & van Heijst, 2002)
- crust: 3D global crustal model by Meier et al. (2007a,b)
- anelastic: smoothed version of QL6 (Durek & Ekström, 1996)

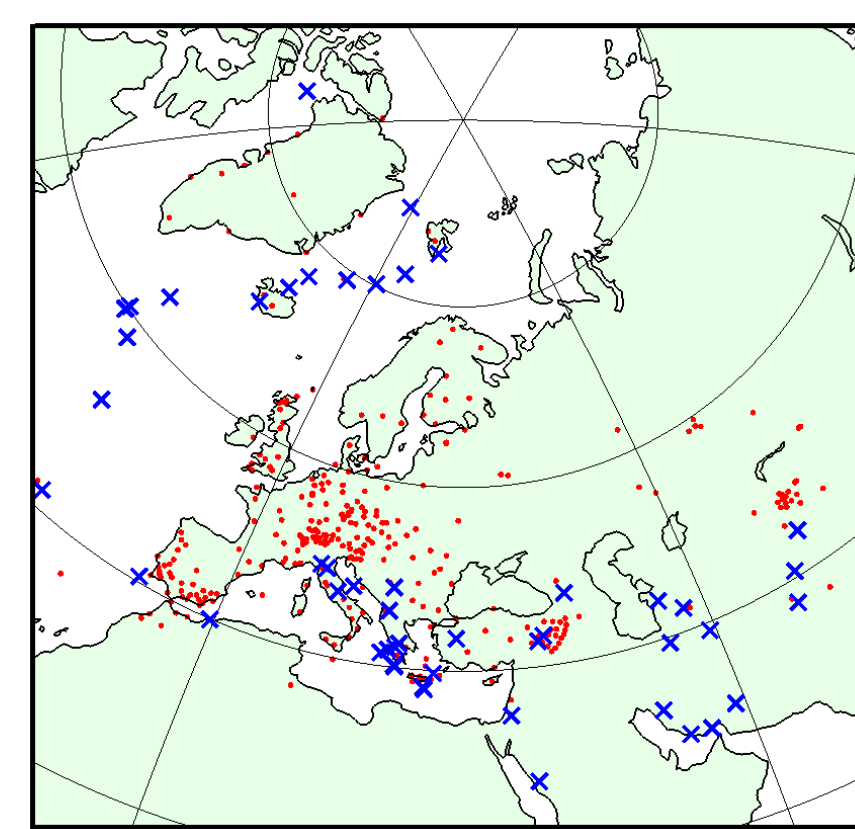


Figure 2: Distribution of sources (blue crosses) and receivers (red dots).

3. The Model preliminary, after 12 iterations

The current model, shown below, is the result of 12 conjugate-gradient iterations with data in the period range from 50-300 s.

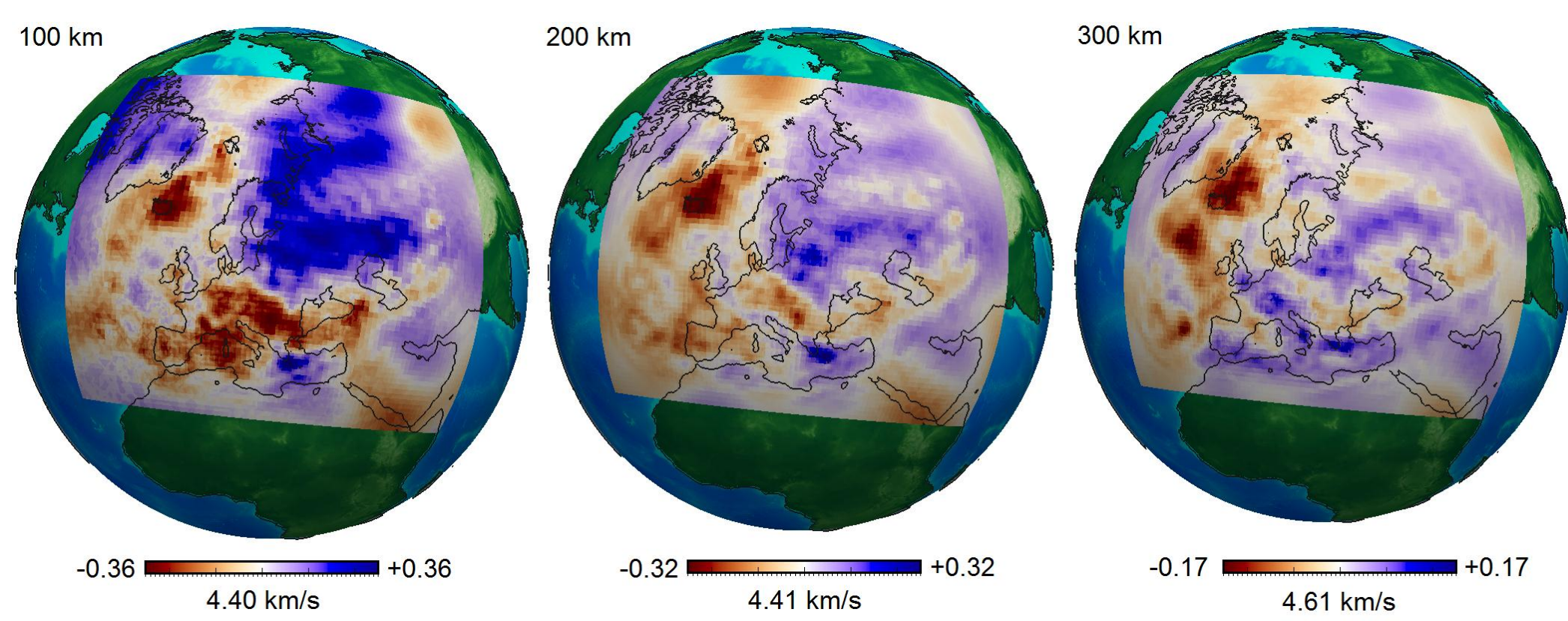


Figure 3: Horizontal slices through the isotropic S velocity distribution at 100 km, 200 km and 300 km depth. Various structural features are clearly visible, e.g. the low velocities of the Iceland hotspot and the Pannonian basin, and the high velocities of the east European platform, the Baltic shield and the Hellenic subduction system.

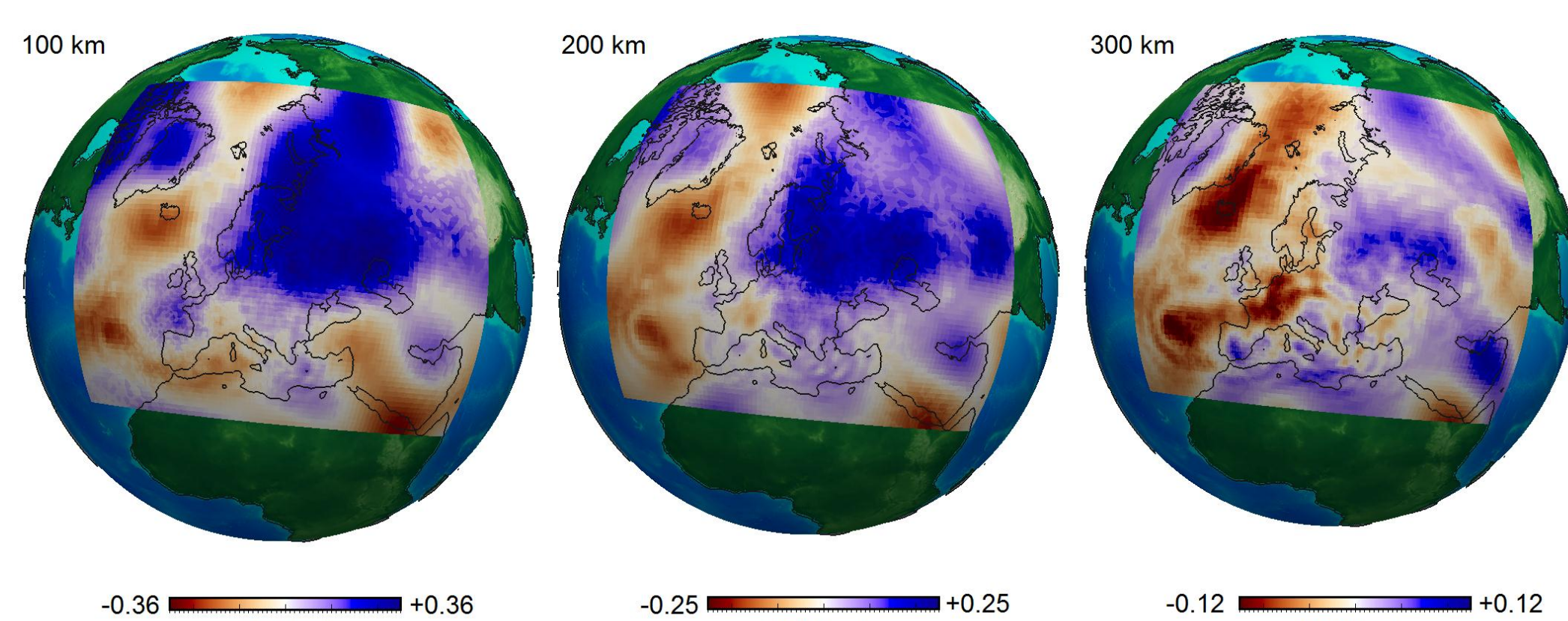


Figure 4: Horizontal slices through the P velocity distribution at 100 km, 200 km and 300 km depth. The P velocity model still closely resembles the initial model, but also reveals an unusually pronounced Iceland plume. Note that the large-scale S and P velocity heterogeneities are not generally correlated.

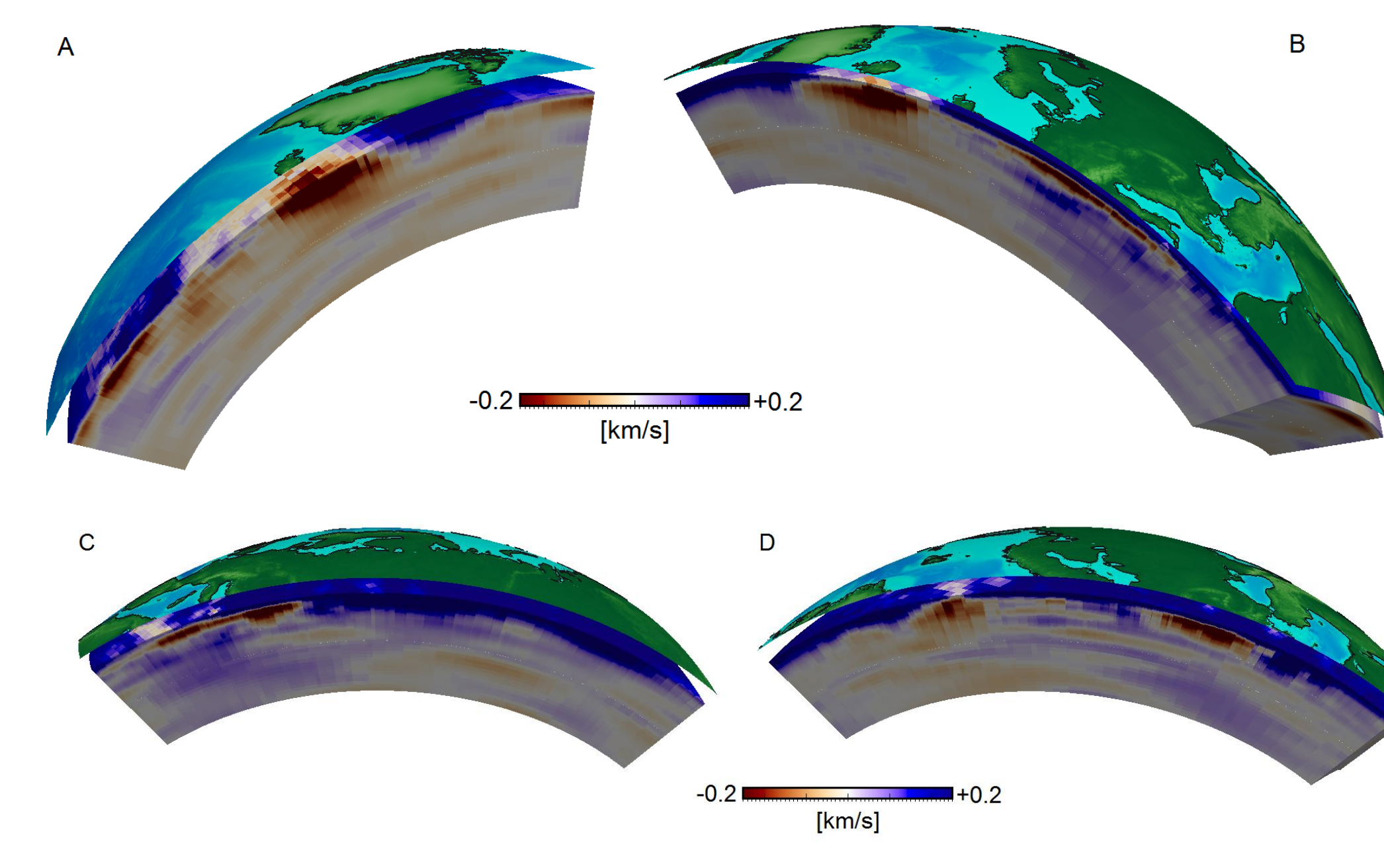


Figure 5: Vertical slices along various profiles indicated in the topographic map below. The models are plotted from 50 km to 1000 km depth. Clearly visible are, for instance, the extremely low velocities beneath the Pannonian basin and the confinement of the Iceland plume to depth above ≈ 600 km.

4. Data fit

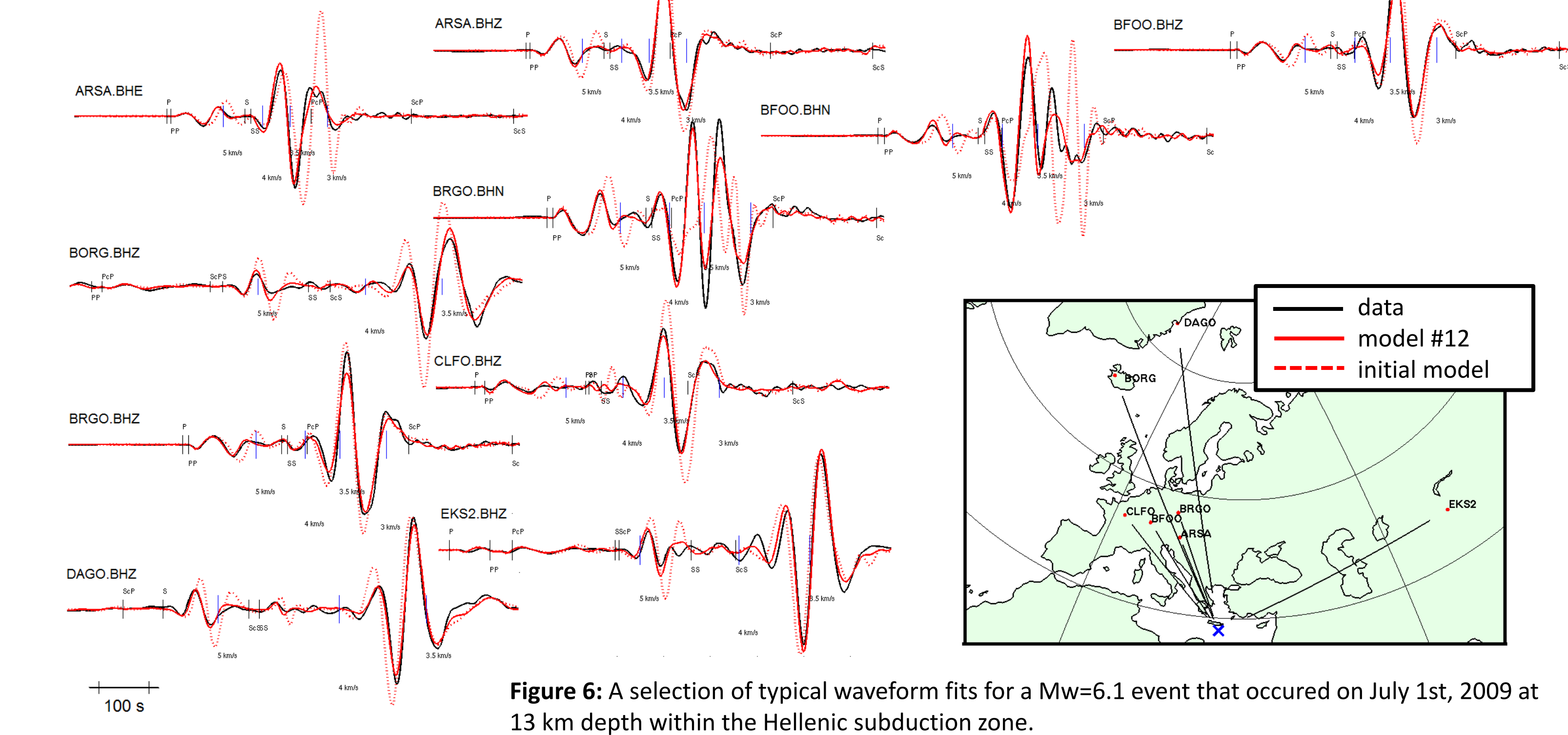


Figure 6: A selection of typical waveform fits for a Mw=6.1 event that occurred on July 1st, 2009 at 13 km depth within the Hellenic subduction zone.

After 12 iterations the **data fit improved substantially**, mostly for paths crossing prominent structural features that are not present in the initial model. These include the Hellenic subduction zone and the Pannonian basin.

Figure 6 shows a collection of waveform comparisons. The **strongest effects** are due to the appearance of the **Hellenic slab** (body waves) and the incorporation **polarisation anisotropy** that accounts for the Love-Rayleigh discrepancy (horizontal-component surface waves).

A summary of the misfit reduction after 12 iterations is shown in figure 7 in the form of phase misfit histograms.

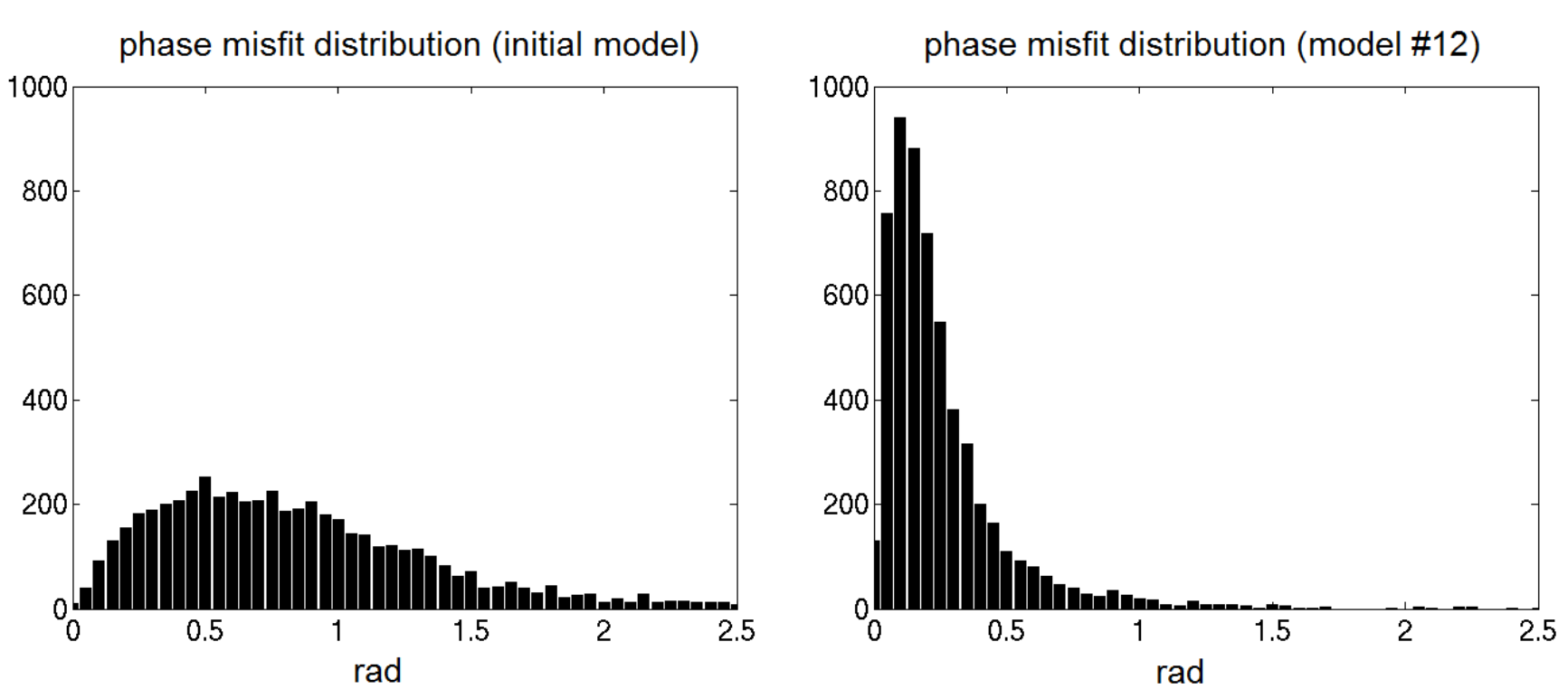


Figure 7: Distributions of the cumulative time-frequency misfit of each seismogram for the initial model (left) and model #12 (right).

5. Resolution analysis preliminary

Resolution analysis in full waveform inversion remains a difficult challenge. It has, so far, mostly been based on visual analysis, synthetic inversions and the inspection of data fit.

The lack of a quantitative means to assess resolution in full waveform inversion has made this technique susceptible to serious criticism. Is it really worth the effort given the enormous computational costs?

To quantify the resolution of full waveform tomographic images, we developed a method based on the computation of Hessian kernels, i.e. the volumetric densities of the second derivatives of the misfit functional (Fichtner & Trampert, 2011a).

This allows us to estimate position- and direction dependent resolution length, as shown in figure 8 (Fichtner & Trampert, 2011b).

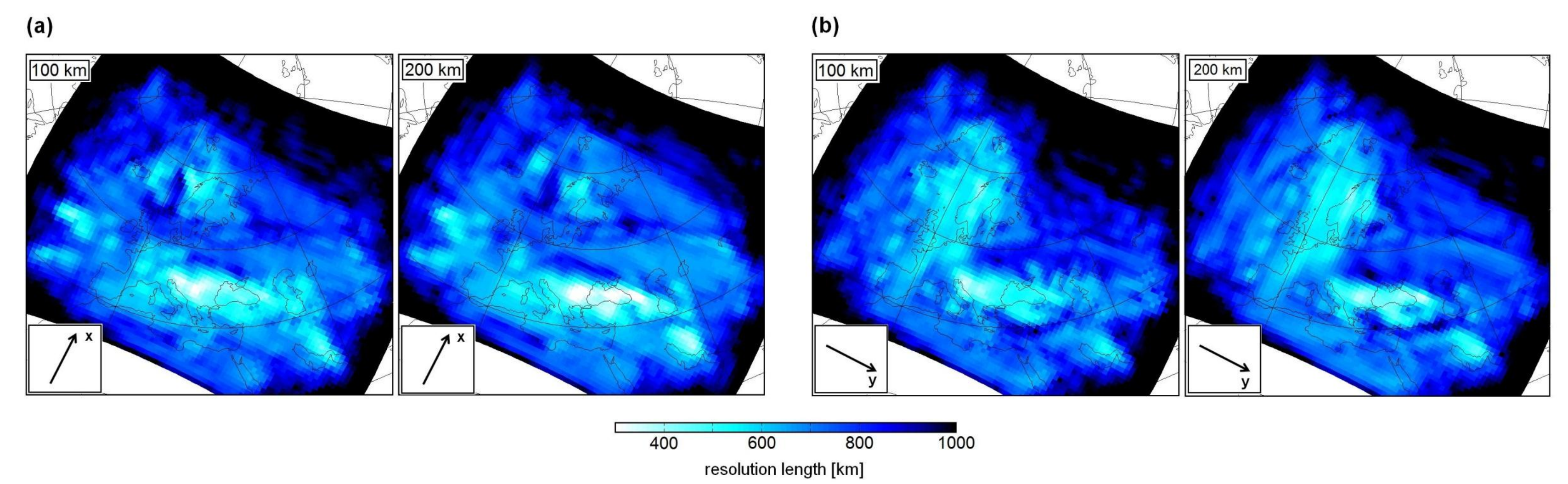


Figure 8: Resolution length at different depths and in different directions, indicated by the arrows. For this analysis we used data in the period range 100-300 s, meaning that it provides a conservative estimate for the model from figures 3 to 5, for which 50-300 s data were used.

6. Predictability

An important diagnostic for the meaningfulness of a tomographic model is its ability to **predict waveforms** that were **not included in the inversion**.

The event shown in the top row of figure 9 is particularly interesting, as its **source is located at ≈ 200 km depth**. The waveforms are well predicted even though **deep events were not used in the inversion**.

As demonstrated in figure 9, our model **predicts both body and surface waveforms**. The accuracy is approximately the same as for the data used to constrain the model.

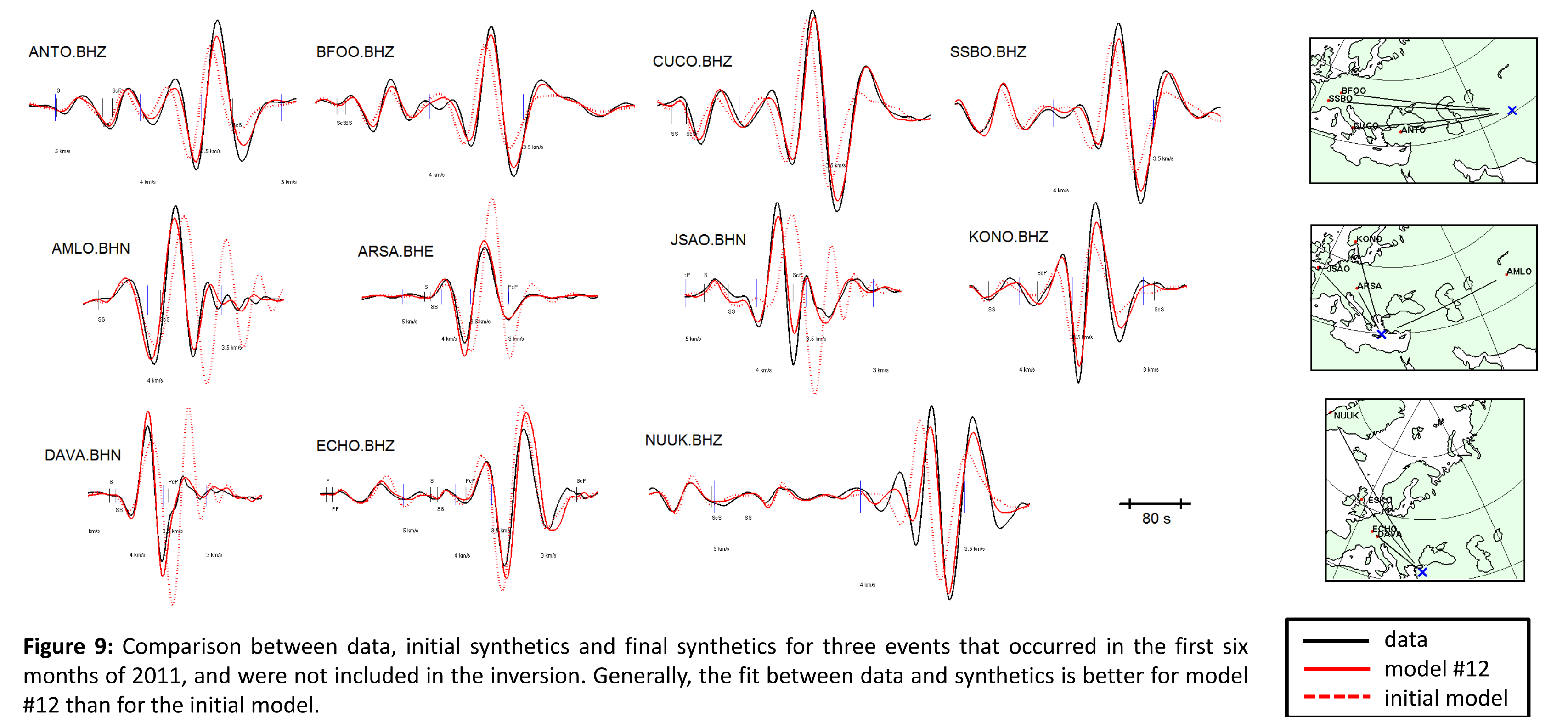


Figure 9: Comparison between data, initial synthetics and final synthetics for three events that occurred in the first six months of 2011, and were not included in the inversion. Generally, the fit between data and synthetics is better for model #12 than for the initial model.

7. Some thoughts on Q

Given the model's capability to explain the arrival times of both body and surface waves, we attempted to **invert amplitude misfits for 3D anelastic structure**.

To our surprise, however, **amplitudes are almost perfectly explained by elastic structure, the source and station corrections**. In many cases the **purely elastic effect** on amplitudes is on the order of **tens of percent** (see figure 10). The remaining misfit leads to a chaotic and rather meaningless update of 3D Q.

It follows that **3D Q cannot be constrained independently with data in the period range from 50 s to 300 s**. A larger bandwidth and near-source data are required.

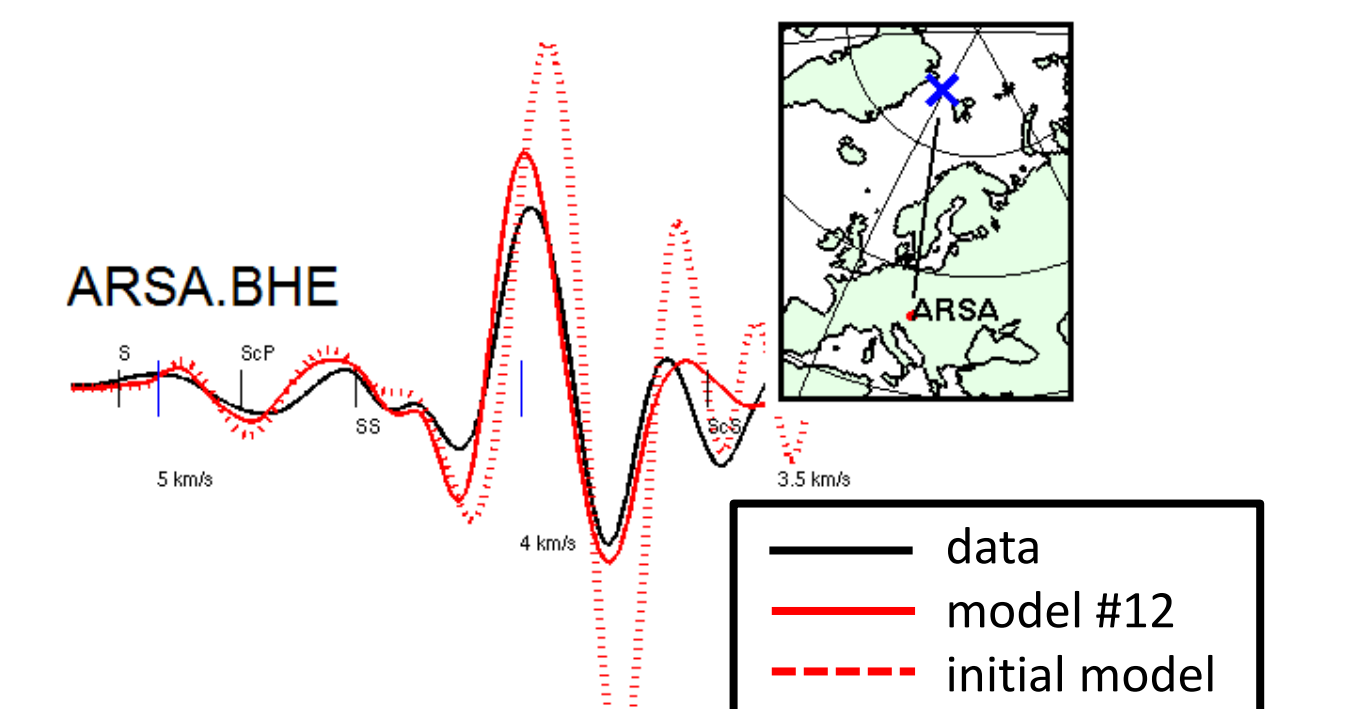


Figure 10: Purely elastic amplitude effect at station ARSA. The dominant period is 80 s.

8. Regional data

The next step in the development of ECOS consists in the incorporation of **regional data sets**, starting with the dense networks of **Spain and Turkey**.

Regionally, the data can be modelled at periods down to ≈ 5 s.

This will provide detailed models of **lithospheric structure**, needed for **finite source studies** and **ground motion prediction**.

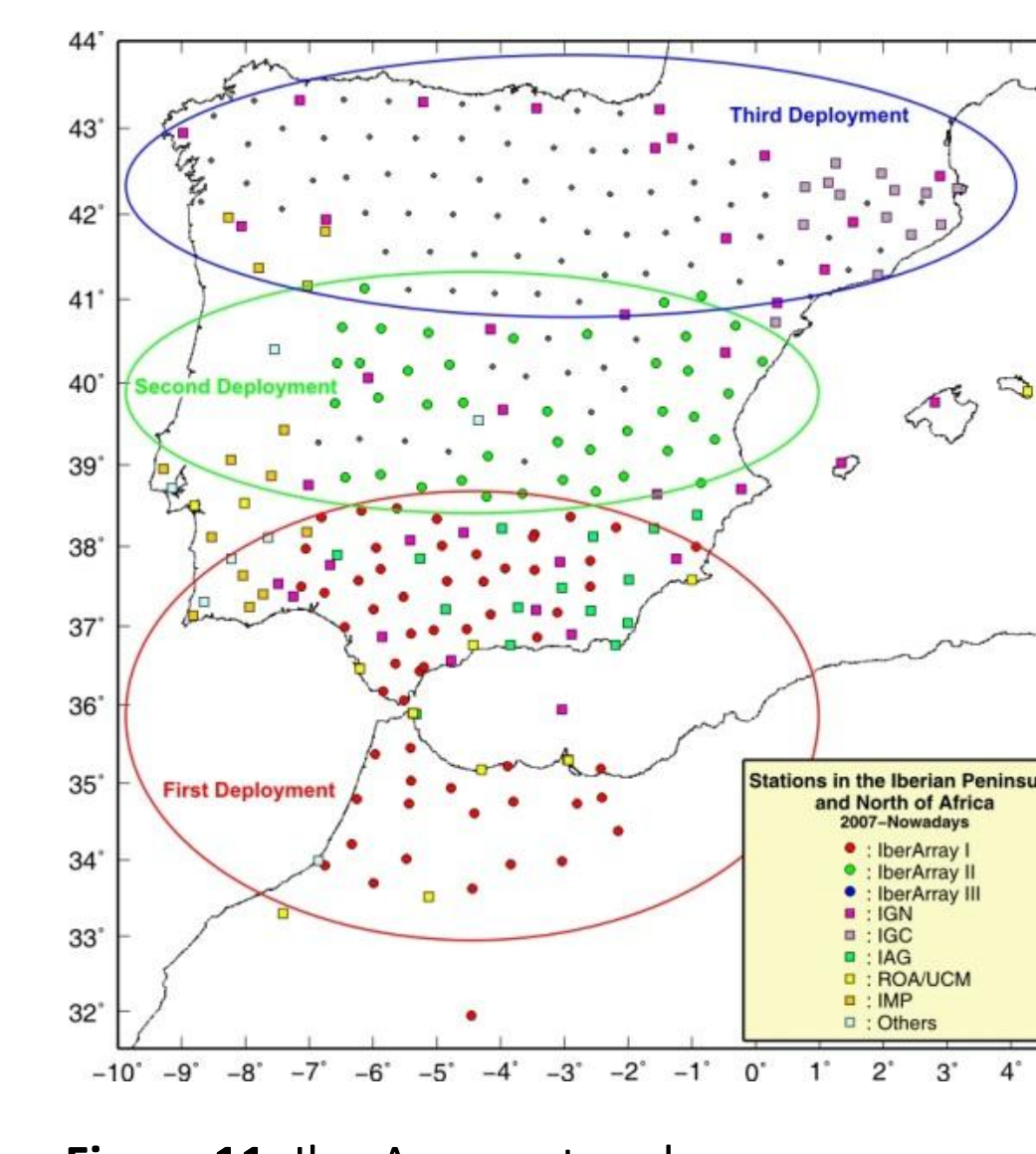


Figure 11: IberArray network.

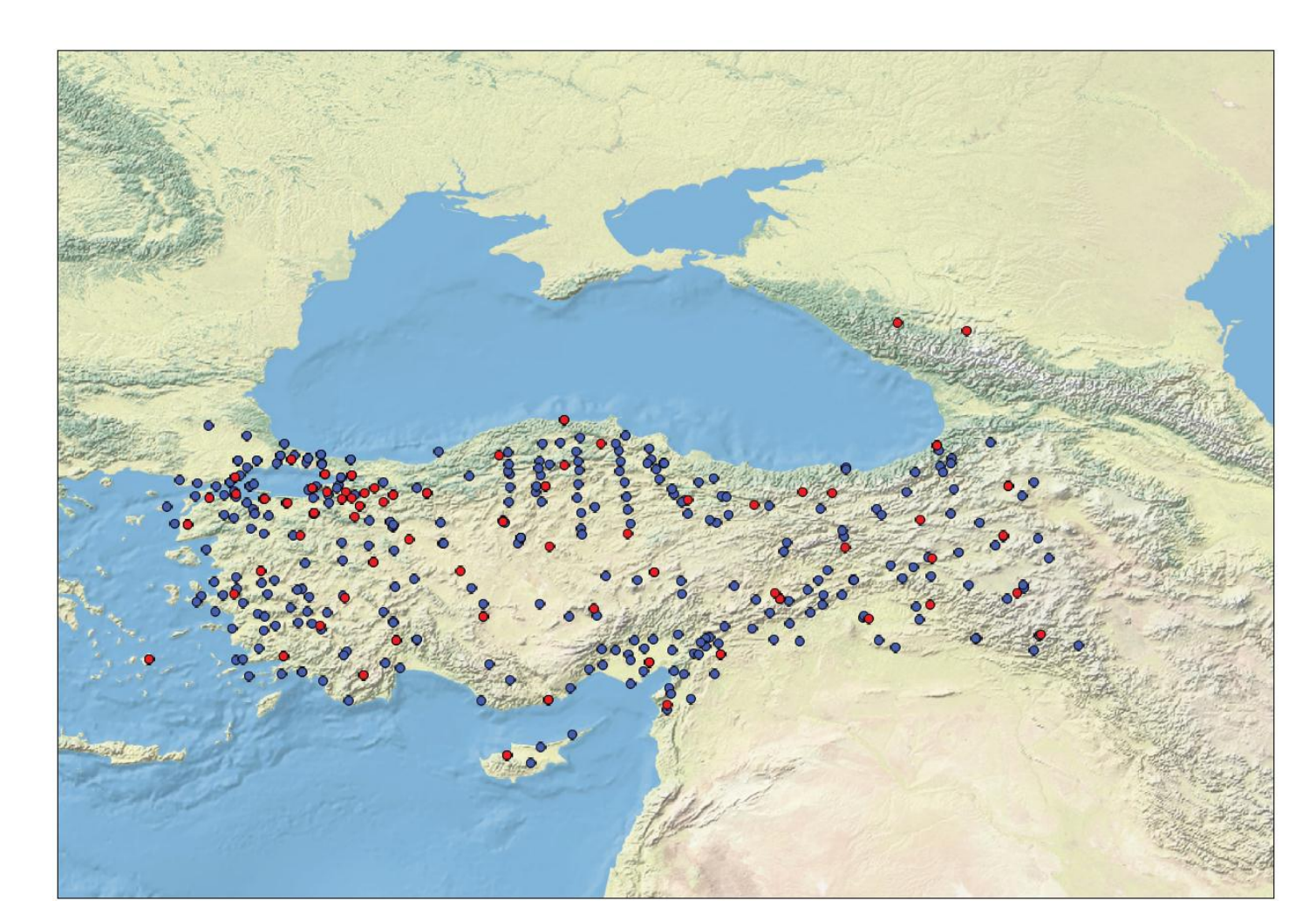
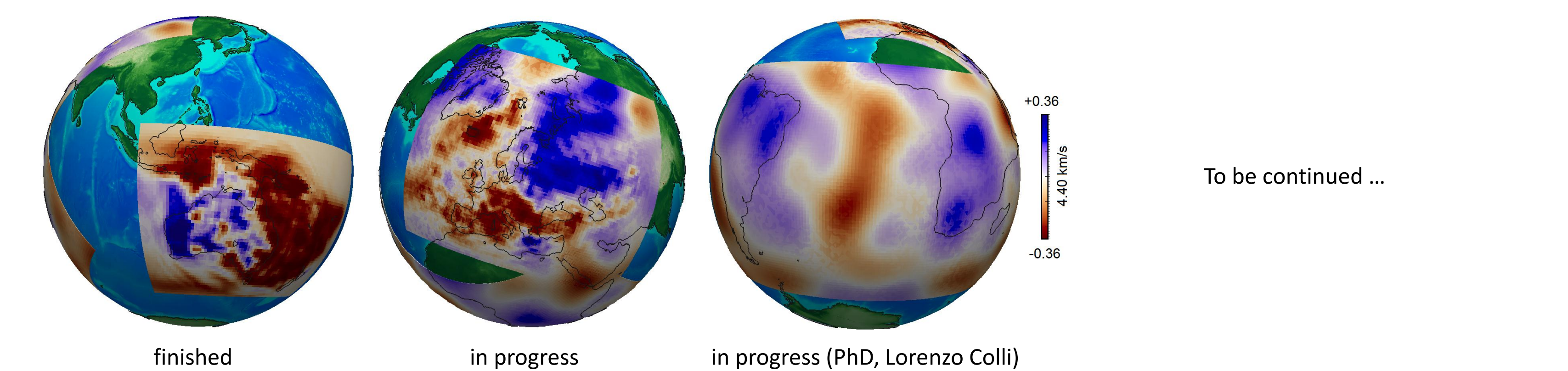


Figure 12: Broad-band (blue) and short-period (red) stations of the Turkish seismometer network.

9. A look further ahead



To be continued ...

References

Amante, C., Eakins, B. W., 2009. ETOPO1: 1 Arc-Minute Global Relief Model: Procedures, Data Sources and Analysis. NOAA Technical Memorandum NESDIS NGDC-24, 19 pp.
 Durek, J. J. & Ekström, G., 1996. A radial model of anelasticity consistent with long-period surface wave attenuation. *Bull. Seis. Soc. Am.*, **86**, 144-158.
 Fichtner, A., Igel, H., 2008. Efficient numerical surface wave propagation through the optimisation of discrete crustal models - a technique based on non-linear dispersion curve matching (DCM). *Geophys. J. Int.*, **173**, 519-533.
 Fichtner, A., Kennett, B.L.N., Igel, H., Bunge, H.-P., 2008. Theoretical background for continental- and global-scale full waveform inversion in the time-frequency domain. *Geophys. J. Int.*, **175**, 665-685.
 Fichtner, A., Trampert, J., 2011a. Hessian kernels of seismic data functionals based upon adjoint techniques. *Geophys. J. Int.*, **185**, 775-798.
 Fichtner, A., Trampert, J., 2011b. Resolution analysis in full waveform inversion. *Geophys. J. Int.*, submitted.
 Meier, U., Curtis, A. & Trampert, J., 2007a. Fully nonlinear inversion of fundamental mode surface waves for a global crustal model. *Geophys. Res. Lett.*, **34**, doi:10.1029/2007GL030989.
 Meier, U., Curtis, A. & Trampert, J., 2007b. Global crustal thickness from neural network inversion of surface wave data. *Geophys. J. Int.*, **169**, 706-722.
 Ritsema, J., van Heijst, H. & Woodhouse, J.M., 1999. Complex shear wave velocity structure imaged beneath Africa and Iceland. *Science*, **286**, 1925-1928.
 Ritsema, J. & van Heijst, H., 2002. Constraints on the correlation of p- and s-wave velocity heterogeneity in the mantle from P, PP, PPP and PKP travel times. *Geophys. J. Int.*, **149**, 482-489.